

Flexible Light Emission Diode Arrays Made of Transferred Si Microwires-ZnO Nanofilm with Piezo-Phototronic Effect Enhanced Lighting

Xiaoyi Li,^{†,§,‡} Renrong Liang,^{‡,†} Juan Tao,[§] Zhengchun Peng,[§] Qiming Xu,[§] Xun Han,[§] Xiandi Wang,[§] Chunfeng Wang,[§] Jing Zhu,^{*,†} Caofeng Pan,^{*,§} and Zhong Lin Wang^{*,§,||}

[†]National Center for Electron Microscopy in Beijing, School of Materials Science and Engineering; The State Key Laboratory of New Ceramics and Fine Processing; Key Laboratory of Advanced Materials (MOE); Center for Nano and Micro Mechanics and [‡]Institute of Microelectronics, Tsinghua University, Beijing 100084, P. R. China

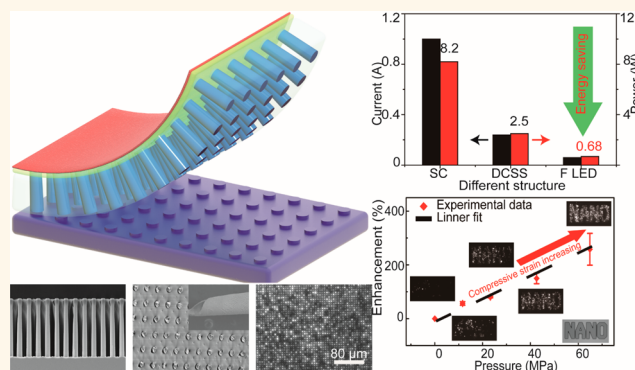
[§]Beijing Institute of Nanoenergy and Nanosystems, Chinese Academy of Sciences; National Center for Nanoscience and Technology, Beijing 100083, P. R. China

^{||}School of Materials Science and Engineering, Georgia Institute of Technology, Atlanta, Georgia 30332-0245, United States

Supporting Information

ABSTRACT: Due to the fragility and the poor optoelectronic performances of Si, it is challenging and exciting to fabricate the Si-based flexible light-emitting diode (LED) array devices. Here, a flexible LED array device made of Si microwires-ZnO nanofilm, with the advantages of flexibility, stability, lightweight, and energy savings, is fabricated and can be used as a strain sensor to demonstrate the two-dimensional pressure distribution. Based on piezo-phototronic effect, the intensity of the flexible LED array can be increased more than 3 times (under 60 MPa compressive strains). Additionally, the device is stable and energy saving. The flexible device can still work well after 1000 bending cycles or 6 months placed in the atmosphere, and the power supplied to the flexible LED array is only 8% of the power of the surface-contact LED. The promising Si-based flexible device has wide range application and may revolutionize the technologies of flexible screens, touchpad technology, and smart skin.

KEYWORDS: ultrathin flexible electronics, piezo-phototronic effect, wire array transfer, silicon microwire array, energy saving



The promising Si-based flexible light-emitting diode (LED) array devices, with the advantages of flexibility, lightweight, energy savings, and high efficiency, can be used as strain sensors to demonstrate the pressure distribution by the differences of light emission intensities, which could revolutionize the current technologies for flexible screens, human-machine interfaces, touchpad technology, personal signatures, and smart skin.¹⁻³ In this work, a flexible LED array device made of transferred Si microcolumns-Zn nanofilm is fabricated and lighted up continuously for more than 24 h and turned on and off for more than 10^{11} times when applied by a pulse voltage with the frequency of 1 MHz. The power supplied to the flexible LED array is only 8% of that of the surface-contact LED (SC LED),¹ shown in Figure 4d or Figure S3. The electroluminescent (EL) intensity of the flexible LED array device is increased more than 3 times when under 60 MPa static compressive strains. A visualized strain/pressure mapping system can be formed just by recording the EL

intensities of the LEDs. With the help of the well-developed Si microelectronic technology, large-scale integrated devices can be easily fabricated for the use of Si-based optical communication systems and photonic integrated circuits,⁴ which will largely increase the speed of data transmission and operation in the future.

RESULTS AND DISCUSSION

Due to their large surface-to-volume ratios, anisotropic electrical conductive properties, good light absorption, and thermal-conductive abilities, as well as the advantages of low cost, abundant sources, and simple fabrication, the vertical silicon wire arrays show promising advances for the applications

Received: January 13, 2017

Accepted: March 31, 2017

Published: March 31, 2017

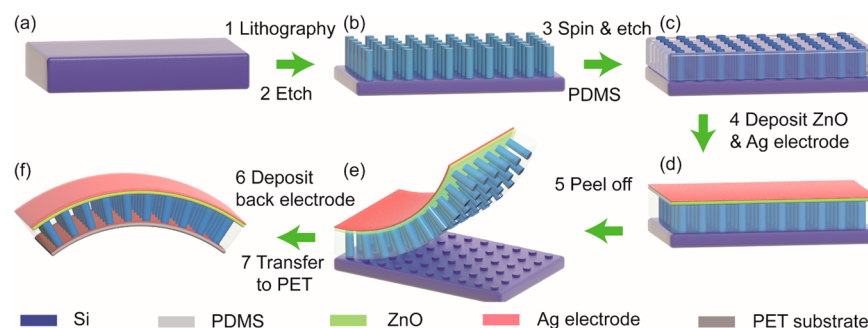


Figure 1. Fabrication process of the flexible polymer/Si/ZnO LEDs array device. (a–e) Diagrams of transfer process of vertical Si microwire arrays. (f) Illustration of the flexible polymer/Si/ZnO LEDs array device.

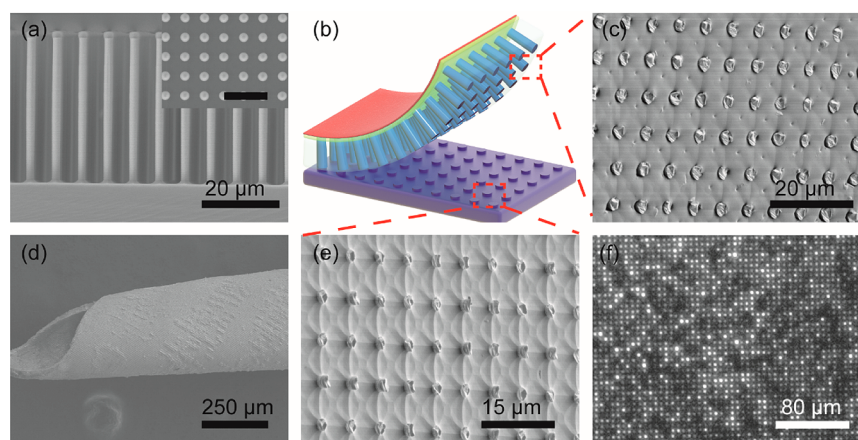


Figure 2. Characterization of the flexible LED array structure. (a) Side view of Si microwires by SEM, and the inset is the top view with a scale bar 15 μm . (b) Schematic diagram of the transferred flexible LED array device and the Si substrate. (c) The back side of the polymer/Si microwire array composite film. (d) The transferred flexible film, rolled into cylinders. (e) SEM image of Si substrate after transfer process. (f) Optical image of the LED array device under 10 V biased voltages.

of vertical devices, for example, field-effect transistors,^{5,6} LEDs,^{7,8} solar cells,^{9,10} biosensors,^{11–13} thermoelectric modules^{14,15} and smart skin.¹ However, there are some big challenges to utilizing the specific optical and electrical properties of the Si wire array device, especially the Si wire-based flexible LED array device. First, as the Si wire array contains billions of wires with a complex pattern, the structure and the pattern of the Si wire array are extremely difficult to maintain during the transfer process. Second, the indirect band gap and the low carrier mobility of Si are existing problems. Finally, due to the immature technology of flexible electrodes, it is almost impossible to ensure that every pixel of the bended flexible LED array will light up. Tremendous efforts have been made to improve the fabrication processes. A range of different methods have been applied to achieve the mechanical breakage and transfer of the Si wire by application of shear forces,¹⁶ peeling forces,¹⁷ or the porous crack of the Si wires.¹⁸ Also, different methods have been attempted, such as energy band engineering, doping with special elements (Er, *etc.*), structure modification (*e.g.*, porous silicon), and piezo-phototronic effects, to improve the EL properties of Si LEDs.

To fabricate the most popular semiconductor in the world in LED, we etched and transferred the Si microwire arrays to produce a flexible n-ZnO/p-Si heterostructure LED array device, featuring high intensity of visible light, flexibility, long lifetime, and energy saving. The fabrication process of the vertical Si microwire array device is demonstrated in Figure 1. P-type Si wafers are cleaned (Figure 1a) and then spin-coated

by photoresist to get the designed pattern through lithographing. After etching, large arrays of Si microwires are formed (Figure 1b).^{1,19} The diameter, length, and center-to-center distance of the Si microwires are 2.5, 40, and 5.5 μm , respectively, indicating that the Si arrays are vertically oriented and well-ordered. Polydimethylsiloxane (PDMS) polymer is used as a matrix to support the microwires to fabricate the mechanically free-standing polymer/Si microwire array composite film (Figure 1c). Then the Si microwire tips are exposed by oxygen plasma etching (Figure S1e). A ZnO nanofilm (200 nm in thickness) is deposited in direct contact with the Si microwires to form a p–n junction (shown in Figure S2), and an Ag layer is used as the top electrode for the entire microwire array (Figure 1d). The polymer/Si microwire array composite film is then peeled off from the Si substrate mechanically, generating a flexible and mechanically free-standing material containing a well-ordered crystalline Si array (Figure 1e). The area of the removed polymer/Si microwire sheet could be $>4 \times 4$ cm, and the size of the flexible film is only limited by how big the Si wafer is. Another Ag nanofilm is evaporated onto the back side of the device to form the ohmic contact. Finally the polymer/Si microwire array composite film is then adhered to a PET substrate (Figure 1f), and the Si substrate can be reused for etching another Si microwire array after polishing. The flexible polymer/Si/ZnO LED array can be uniformly lit up under a bias of 10 V, and each microwire is a single light emitter. The light emission

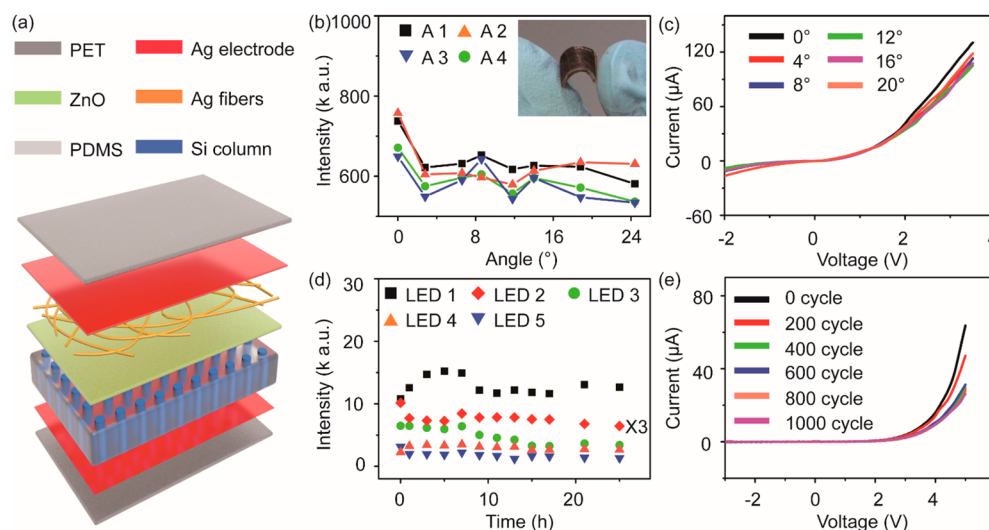


Figure 3. Flexibility of flexible LED array device. (a) Schematic structure of the flexible LED array device. Light emission intensities of different areas of (b) LEDs and (c) I - V curves under different bending angles. (d) The light emission intensities of different LEDs when lighted up continuously for more than 24 h powered by a pulse voltage with the frequency of 1 MHz. (e) Mechanical stability of the flexible LED array device for 1000 cycles.

intensity of the LEDs can be increased when under compressive strains.

Cross-sectional and top scanning electron microscopy (SEM) images of the silicon microwire array are presented in Figure 2a, showing a length of 40 μm and diameter of 2 μm for the Si columnar structure. After it is peeled off from the Si substrate, the back side of the polymer/Si microwire array composite film is presented in Figure 2b,c, revealing the gapless structure of the PDMS matrix and the microwires. Figure 2c also shows that the tips of the Si microwires are uncovered, permitting the subsequent ohmic contact with the electrodes. The as-removed polymer/Si microwire array composite film can be folded into cylinders whose diameters can be smaller than 100 μm (Figure 2d) without significant displacement or damages. The polymer/Si microwire array composite film also keeps the orientation, spacing, pattern, and unit of the array.²⁰ The microwires in such film present electrical conduction from top side to back side while being highly isolated laterally. The SEM image of the Si substrate after the transfer process is illustrated in Figure 2e, demonstrating all the Si microwires have been perfectly removed. Light emission of the polymer/Si microwire arrays/ZnO device, when applied at 10 V, is presented in Figure 2f, which shows that each microwire is a single light emitter. The difference between each individual LED's emission intensity is explained as the nonuniform distribution of serial contact resistances. When introducing a bar electrode or Ag wire network electrode (Figure 3a), better performances and more uniform light emission can be obtained, since the distribution of contact resistances problem is effectively eliminated with the advanced designs.

Through the method described above, different shapes and different lengths of the Si microwires can be obtained. Efforts have been made to achieve better structure for the mechanical breakage and transfer of the Si microwires. In Figure S1a, the top of the Si microwire is much wider than the bottom, which makes mechanical breakage and separation of the Si microwires much easier. The method maintains the pattern and the structure of the Si microwire arrays during the transfer process. Because the Si microwire length can be controlled, ultrathin polymer/Si composited film can be as thin as 8 μm (Figure

S1b,c), which significantly reduces the thickness of the whole device and increases the potential applications of the ultrathin device.

Our method of transfer has five key merits. First, the method can be applied broadly, regardless of the dimensions, lengths, materials, and fabricating methods of the Si wires. Figure 2 and Figure S1 demonstrate that this method can apply to Si microwires ranging from 8 to 40 μm in length. Second, the orientation, structure, and pattern of Si microwire arrays are well-kept during the transfer process. Even patterned arrays containing billions of Si microwires (Figure 2c,d) can be perfectly transferred, keeping the shape of the pattern. Third, Si wafers can be repeatedly used to etch vertical Si microwire arrays. Usually, when the Si microwire array is transferred, the Si substrate may be wasted. To make the best use of the Si material, the remaining Si substrate after polishing is reutilized and etched to create a second Si microwire array layer. The structure of the second Si array layer is the same as that manufactured on the original Si wafer. The thickness of a commercial Si wafer is approximately 500 μm , although approximately 40 μm height of Si is abraded in each polishing process, the wafer could still be re-etched up to about 10 times for the 8 μm Si microwire array. Therefore, the reutilization of the remaining Si wafer substrate is extremely important and economical. The fourth merit of this method is that the polymer/Si microwire array composite film can be transferred to most flat substrate, like glass, metal, polymer film, and so on. The fifth merit is that the Si microwire array can be used to fabricate different kinds of devices, such as LEDs, solar cells, optical detectors, and so on, with a designated thickness. It will largely promote the application of the ultrathin device.

The flexible polymer/Si/ZnO LED array device is completed by sandwiching the polymer/Si layer between a ZnO depositing layer and the electrodes (Figure 3a). As is generally understood, it is challenging to fabricate a flexible electrode with high conductivity, especially to make sure the billions of LEDs in the array maintain good contact with the electrodes on both sides when the device is bent. Even a single LED in the array has poor contact with the electrode, the screen based on the LED array will have a missing pixel and appear imperfect. A great

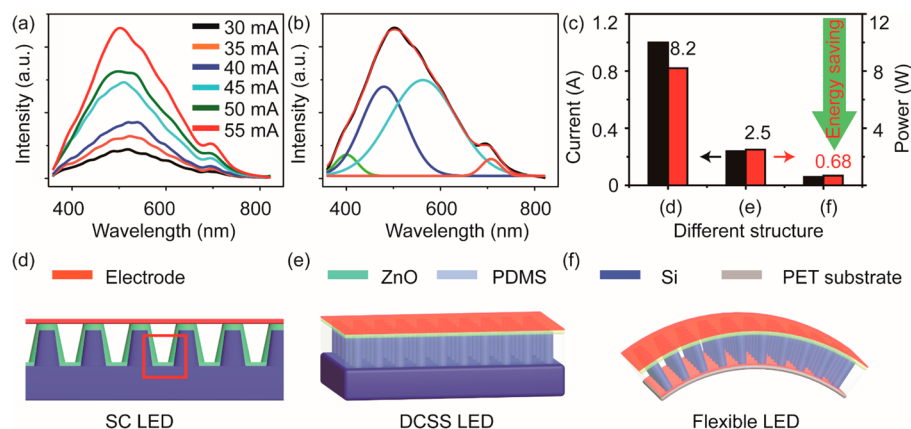


Figure 4. Light emission performances of the flexible LED array device. (a) EL spectra of the flexible device under different input currents. (b) Gaussian functions were used to deconvolute the peak of the spectrum when the input current is 30 mA. (c–f) Comparison between three different similar structures of ZnO/Si LED array devices: (d) SC LED, (e) DCSS, and (f) flexible LED.

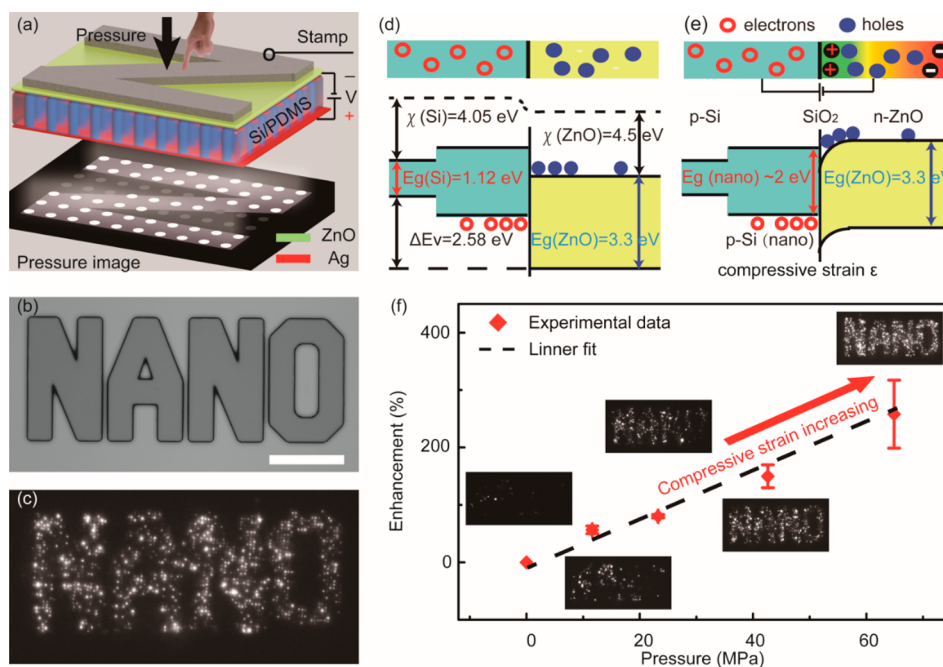


Figure 5. Working mechanism and enhancements by piezo-phototronic effect. (a) Working mechanism of the pressure distribution function of the flexible LED array device. (b) A patterned sapphire stamp shaped to read “NANO” with a scale bar 150 μm . (c) Pressure distribution mapping by the LED array as the word “NANO”. (d) Energy band of the flexible LEDs array device under no stains nor bias voltages and (e) band under a bias voltage and compressive strains. (f) Pressure distribution mapping under different pressure by the LEDs array intensity image.

many researchers have devoted themselves to improving the conductive properties of the flexible electrodes in recent years. Here we add a layer made of Ag fibers to ensure that the majority of LEDs in the array will still light well even when the device is bent.²¹ In order to study the flexibility of the LED array device before and while being bent, the intensity and I – V curves of the LED array device are measured under different bending angles. Figure 3b shows the relationship of the intensity of the LEDs with the bending angle, which reveals that the intensity of the LEDs will slightly decrease and then remain stable as the bending angle increases. The inset of Figure 3b shows the flexible LED array device is quite flexible and can be bent to a large angle. No significant deviation of the I – V curves is observed, as shown in Figure 3c, which indicates that the array device possesses excellent flexibility. Also the Si

microwires and the ZnO nanofilm consist of billions of p–n junctions and show a clear rectifying behavior, indicating the formation of diodes.²²

Meanwhile, the flexible device is stable. Figure 3d reveals the LEDs can be lighted up continuously for more than 24 h when applied by a pulse voltage with the frequency of 1 MHz. Considering the indirect band gap of the Si materials, most Si-based LEDs have difficulty emitting light and generate large amounts of heat due to low efficiency. The flexible LED device has a longer lifetime. During the testing, the LEDs are turned on and off for more than 10^{11} times. The device can still be lighted up after 6 months (placed in the atmosphere), indicating the excellent stability of the device.

To better understand the mechanical flexibility, the long-term stability of the flexible LED array device for 1000 cycles at

a 45-degree bending angle was measured (Figure 3e). The flexible LED array device shows good durability.²³ The I - V curves decrease at first and remain almost constant during hundreds of bending cycles, indicating the flexible LED array device can still light up even after 1000 bending cycles. The initial decreases are most likely caused by the small separation between the interface of the device and the electrode when bending, as the device recovers when releasing without noticeable failure and has good repeatability. The cycling stability, mechanical flexibility, and long lifetime of the flexible LED array device will be beneficial for their practical applications.

The EL emission spectra of the flexible LED array device is obtained when the input current increases (30, 35, 40, 45, 50, and 55 mA) at room temperature, Figure 4a. When the input current increases, the EL intensity becomes higher, and the peak positions of different currents are similar. To better explain the physical mechanism of light emissions, Gaussian function is applied to deconvolute the peaks, as seen in Figure 4b. Four distinct peaks can be simulated from the emission spectra, and each corresponds to a particular recombination mechanism as mentioned. The schematic band diagram of the ZnO-Si heterostructure is shown in Figure 5d. The peak near 400 nm in Figure 4b is the near-band emission of ZnO.^{24,25} The peak around 500 nm and the peak near 600 nm are related to the defects emission in ZnO nanofilm.^{26–29} Because of the nano and microstructures at the surface of the Si microwires (Figure S1f), the energy band gap of Si with nano/microstructures near the heterojunction interface is bigger than that of bulk Si,¹ which is associated with the peak of 700 nm.^{8,30–32}

As Si is an indirect bandgap semiconductor, the excited charged carrier in silicon will be scattered to the electronic branch and relaxes along the electronic branch by scattering with phonons (Figure S4e).³³ Both energy and momentum must be conserved, thus the emitted photon will have energy E .

$$E = E_{\text{excited}} - \sum E_{\text{scattering}} \quad (1)$$

where E_{excited} is the excitation energy, and $\sum E_{\text{scattering}}$ is the total energy of all scattering phonons. The lifetime of the intraband relaxation in silicon is approximately 1 ps, while the radiative recombination occurs on a 10 ns time scale. Therefore, the radiative recombination occurs normally. On the other hand, the relaxation of intraband will generate the phonons with the momentum \mathbf{q} , and finally convert the energy ($\sum E_{\text{scattering}}$) into heat. This phenomenon results in low efficiency, a great quantity of energy wasted, and a large amount of heat.

However, there are three reasons to explain why the flexible LED array device is energy saving. First, the Si/ZnO contact area of dot-contact LED is only about 13.63% of that of the SC LED. A comparison between three different Si/ZnO structures is shown in Figure 4c–f. In Figure 4d the ZnO nanofilm forms surface contact with the Si microwires, meaning the SC LED has a larger contact area than the dot-contact with Si substrate LED (DCSS LED) in Figure 4e and flexible LED in Figure 4f. The additional contact surface is marked by the red rectangle in Figure 4d. Meanwhile, the experiment results demonstrate that light is only generated from the region near the top surface of the Si microwires, and the currents flowing through the surfaces marked in the red rectangle are mostly converted to heat. Second, the Si substrate under the microwire arrays generates a large amount of heat and decreases the efficiency of the LED.

The thickness or the volume of the Si substrate is much larger than that of the Si microwire array, resulting in more energy wasted by the Si substrate. Third, most of the recombination occurs at the ZnO of the flexible LED, which significantly improves the emission efficiency and reduces the heat generated from the photons in the Si material. The emission peaks related to ZnO (near 400, 500 and 600 nm) have a high proportion of the whole emission, and the only peak related to Si is much lower than that of SC LED. In addition, the emission spectra of SC LED have the emission peaks around 780 and 820 nm, which increases significantly when the current reaches at about 0.8A.¹ The method of the flexible LED uses silicon as the p-type material to form the p–n junction and limits the problems of the indirect band and the corresponding low efficiency. Because of the dot-contact and lack of Si substrate, the flexible LED array device will have the highest efficiency theoretically, which corresponds to the experimental results shown in Figure 4c. Figure 4c gives the current and the power when the light intensities of different structure LEDs are almost the same (more information is shown in Figure S3). It is obvious that the flexible structure shown in Figure 4f needs minimum power, and the power supplied to the flexible LED array is only 8% of that of the SC LED in Figure 4d.

A patterned sapphire stamp (NANO), as shown in Figure 5b, was used to apply pressure to the flexible polymer/Si/ZnO LED array device to test the impact of the piezo-phototronic effect. The pressure could be controlled step by step when using the three-dimensional stage shown in Figure 54. The emission of the LEDs when applied by compressive pressure will be enhanced by the piezo-phototronic effect;^{2,34–37} therefore a two-dimensional mapping of pressure was obtained, as shown in Figure 5c,f. Figure 5c shows that the LED intensity image can clearly demonstrate the pressure distribution applied to the LED array as the word “NANO”, which corresponds to the sapphire stamp.^{25,38} Different pressures of 11, 23, 42, and 65 MPa were studied to reveal the relationship between the light intensity and the pressure in Figure 5f. The stronger the pressure applied, the stronger the light intensity obtained, which demonstrates a linear dependence of the light intensity on the pressure.³⁹ Only the LEDs compressed by the patterned stamp change, while those not affected by the patterned stamp show negligible change. No crosstalk of the adjacent pixels is observed, and the resolution of the LED array is 2 μm , shown in Figure S4d, which indicates a reliable resolution of the LED array. Because the center-to-center distance between two neighboring LEDs is 5.2 μm , the flexible LED array device can be used as a 4300 dpi high-resolution pressure mapping system, which shows potential for touchpad technology, personalized signatures, and smart skin.

The schematic band drawings of ZnO/Si heterostructure, shown in Figure 5d,e, illustrate the piezo-phototronic effect and the emission enhancement mechanism. Because of the noncentral symmetry of ZnO, the relative displacement of centers of anions and cations will occur when applied by a compressive strain. When the $+c$ -axis is pointing from the p–n junction interface to the interface of the electrode side, the positive charges of piezoelectricity are generated at the p–n interface, which modify the ZnO's valence and conduction band near the interface, as shown in Figure 5e, and then influence the carriers' actions, such as separation, transport, and recombination. More electrons from the ZnO conduct band and holes from the Si valence band will be trapped at the p–n interface, thus the recombination between holes and electrons

at the interface is raised, which causes the LED's light emission enhancement. Meanwhile, under compressive strains, the potential of the corresponding piezoelectric charges is opposite to the built-in electric field's direction and will reduce the width of depletion region and thus enlarge the injection current and the emission intensity.

CONCLUSIONS

In summary, we designed and manufactured the Si microwire arrays to produce flexible n-ZnO/p-Si heterostructure LEDs at room temperature, featuring high intensity of visible light, flexibility, a long lifetime, and energy savings. The LED array, with good mechanical flexibility, can be lighted up continuously for more than 24 h and turned on and off for more than 10^{11} times when applied by a pulse voltage with the frequency of 1 MHz. A huge amount of energy can be saved when comparing the flexible LED array with SC LED. The EL intensity of the flexible LED array device is enlarged more than 3 times when under 60 MPa compressive strains. A visualized strain/pressure mapping can be formed by recording the EL intensities of the LEDs, which has a wide range of applications and will lead to special optoelectronic devices.

METHODS

Fabrication Process of Si Microwires. P-type Si wafer was cleaned with acetone and dried in nitrogen blow down. The remaining organics and oxide on the Si surface were removed by immersing the Si wafer in hydrofluoric acid (HF, 1%) for 2 min. After the wafer was dried by N_2 for 30 min and treated by hexamethyl disilazane (HMDS) for 10 min, the photoresist (SUN 9i 50 cP) was spin-coated and exposed to form the photoresist pattern. Then, the aligned microwire arrays were generated by the inductive plasma reactive ion etching (SENTECH SI 500). When etching, SF_6 and C_4F_8 gases were applied at the rate of 200 sccm each.

Fabrication Process of the Flexible LED Array. The Si microwires were embedded into a polymer matrix (polydimethylsiloxane (PDMS)), and a curing agent was mixed in a 10:1 w/w ratio. The device was then etched by oxygen plasma etching (SENTECH SI 500) to make sure the ends of the Si microwires were exposed. The ZnO nanofilm (60 W 45 min) and Ag layers (80 W 2–3 min) were deposited by magnetron sputtering (Discovery 635, Denton Vacuum) to form the n-type layer and the electrodes. The flexible polymer/Si microwire array/ZnO composite film was peeled off from the Si wafer mechanically with a sharp blade. Finally, an electrode was deposited on the back side of the flexible polymer/Si microwire array/ZnO composite film.

Characterization and Measurement of the Flexible LED Array. The field-emission scanning electron microscopy Hitachi SU8020 was used to characterize the flexible ZnO/Si LED array device. The Maynuo DS Source M8812 and the pulse power supply Agilent AFG 3011C were used to power the flexible LED array device. The optical images and the emission spectra of the device were measured by Zeiss Observer Z1 and spectrometer Horiba iHR550, respectively. I - V curves were taken by KEITHLEY 4200SCS.

ASSOCIATED CONTENT

Supporting Information

The Supporting Information is available free of charge on the ACS Publications website at DOI: 10.1021/acsnano.7b00272.

Figure S1–S4 showing the structure of different length of the Si microwire array, characterizing the ZnO nanofilm, comparison of different structure of LED array device, and experimental setup (PDF)

AUTHOR INFORMATION

Corresponding Authors

*E-mail: jzhu@mail.tsinghua.edu.cn.

*E-mail: cfp@binn.cas.cn.

*E-mail: zlwang@gatech.edu.

ORCID

Caofeng Pan: 0000-0001-7693-5388

Zhong Lin Wang: 0000-0002-5530-0380

Author Contributions

[‡]These authors contributed equally to this work.

Notes

The authors declare no competing financial interest.

ACKNOWLEDGMENTS

The authors are thankful for support by Chinese National Natural Science Foundation (nos. 51622205, 61675027, 61405040, 51432005, 61505010, 51502018, 11374174, 51390471, and 51527803); National 973 Project of China (2015CB654902); national key research and development project from Minister of Science and Technology, China (2016YFA0202703, 2016YFB0700402 and 2016YFA0302300); and the “Thousand Talents” program of China for pioneering researchers and innovative teams. This work made use of the resources of the National Center for Electron Microscopy in Beijing, Tsinghua National Laboratory for Information Science and Technology and Beijing Institute of Nanoenergy and Nanosystems, Chinese Academy of Sciences.

REFERENCES

- (1) Li, X. Y.; Chen, M. X.; Yu, R. M.; Zhang, T. P.; Song, D. S.; Liang, R. R.; Zhang, Q. L.; Cheng, S. B.; Dong, L.; Pan, A. L.; Wang, Z. L.; Zhu, J.; Pan, C. F. Enhancing Light Emission of ZnO-Nanofilm/Si-Micropillar Heterostructure Arrays by Piezo-Phototronic Effect. *Adv. Mater.* **2015**, *27*, 4447–4453.
- (2) Pan, C. F.; Yu, R. M.; Niu, S. M.; Zhu, G.; Wang, Z. L. Piezotronic Effect on the Sensitivity and Signal Level of Schottky Contacted Proactive Micro/Nanowire Nanosensors. *ACS Nano* **2013**, *7*, 1803–1810.
- (3) Wang, X.; Zhang, H.; Yu, R.; Dong, L.; Peng, D.; Zhang, A.; Zhang, Y.; Liu, H.; Pan, C.; Wang, Z. L. Dynamic Pressure Mapping of Personalized Handwriting by a Flexible Sensor Matrix Based on the Mechanoluminescence Process. *Adv. Mater.* **2015**, *27*, 2324–2331.
- (4) Almeida, V. R.; Barrios, C. A.; Panepucci, R. R.; Lipson, M. All-Optical Control of Light on a Silicon Chip. *Nature* **2004**, *431*, 1081–1084.
- (5) Weisse, J. M.; Lee, C. H.; Kim, D. R.; Zheng, X. L. Fabrication of Flexible and Vertical Silicon Nanowire Electronics. *Nano Lett.* **2012**, *12*, 3339–3343.
- (6) Lugstein, A.; Steinmair, M.; Henkel, C.; Bertagnolli, E. Scalable Approach for Vertical Device Integration of Epitaxial Nanowires. *Nano Lett.* **2009**, *9*, 1830–1834.
- (7) Ball, P. Let There Be Light. *Nature* **2001**, *409*, 974–976.
- (8) Canham, L. Gaining Light from Silicon. *Nature* **2000**, *408*, 411–412.
- (9) Brittman, S.; Gao, H. W.; Garnett, E. C.; Yang, P. D. Absorption of Light in a Single-Nanowire Silicon Solar Cell Decorated with an Octahedral Silver Nanocrystal. *Nano Lett.* **2011**, *11*, 5189–5195.
- (10) Kelzenberg, M. D.; Boettcher, S. W.; Petykiewicz, J. A.; Turner-Evans, D. B.; Putnam, M. C.; Warren, E. L.; Spurgeon, J. M.; Briggs, R. M.; Lewis, N. S.; Atwater, H. A. Enhanced Absorption and Carrier Collection in Si Wire Arrays for Photovoltaic Applications. *Nat. Mater.* **2010**, *9*, 368–368.
- (11) Wang, Y.; Zhang, X. J.; Gao, P.; Shao, Z. B.; Zhang, X. W.; Han, Y. Y.; Jie, J. S. Air Heating Approach for Multi Layer Etching and Roll-to-Roll Transfer of Silicon Nanowire Arrays as SERS Substrates for

High Sensitivity Molecule Detection. *ACS Appl. Mater. Interfaces* **2014**, *6*, 977–984.

(12) Dagdeviren, C.; Yang, B. D.; Su, Y. W.; Tran, P. L.; Joe, P.; Anderson, E.; Xia, J.; Doraiswamy, V.; Dehdashti, B.; Feng, X.; Lu, B. W.; Poston, R.; Khalpey, Z.; Ghaffari, R.; Huang, Y. G.; Slepian, M. J.; Rogers, J. A. Conformal Piezoelectric Energy Harvesting and Storage from Motions of The Heart, Lung, and Diaphragm. *Proc. Natl. Acad. Sci. U. S. A.* **2014**, *111*, 1927–1932.

(13) Hwang, G. T.; Byun, M.; Jeong, C. K.; Lee, K. J. Flexible Piezoelectric Thin-Film Energy Harvesters and Nanosensors for Biomedical Applications. *Adv. Healthcare Mater.* **2015**, *4*, 646–658.

(14) Boukai, A. I.; Bunimovich, Y.; Tahir-Kheli, J.; Yu, J. K.; Goddard, W. A.; Heath, J. R. Silicon Nanowires As Efficient Thermoelectric Materials. *Nature* **2008**, *451*, 168–171.

(15) Hochbaum, A. I.; Chen, R. K.; Delgado, R. D.; Liang, W. J.; Garnett, E. C.; Najarian, M.; Majumdar, A.; Yang, P. D. Enhanced Thermoelectric Performance of Rough Silicon Nanowires. *Nature* **2008**, *451*, 163–167.

(16) Triplett, M.; Nishimura, H.; Ombaba, M.; Logeeswaran, V. J.; Yee, M.; Polat, K. G.; Oh, J. Y.; Fuyuki, T.; Leonard, F.; Islam, M. S. High-Precision Transfer-Printing and Integration of Vertically Oriented Semiconductor Arrays for Flexible Device Fabrication. *Nano Res.* **2014**, *7*, 998–1006.

(17) Spurgeon, J. M.; Boettcher, S. W.; Kelzenberg, M. D.; Brunschwig, B. S.; Atwater, H. A.; Lewis, N. S. Flexible, Polymer-Supported, Si Wire Array Photoelectrodes. *Adv. Mater.* **2010**, *22*, 3277–3281.

(18) Weisse, J. M.; Lee, C. H.; Kim, D. R.; Cai, L. L.; Rao, P. M.; Zheng, X. L. Electroassisted Transfer of Vertical Silicon Wire Arrays Using a Sacrificial Porous Silicon Layer. *Nano Lett.* **2013**, *13*, 4362–4368.

(19) Pan, C. F.; Luo, Z. X.; Xu, C.; Luo, J.; Liang, R. R.; Zhu, G.; Wu, W. Z.; Guo, W. X.; Yan, X. X.; Xu, J.; Wang, Z. L.; Zhu, J. Wafer-Scale High-Throughput Ordered Arrays of Si and Coaxial Si/Si_{1-x}Ge_x Wires: Fabrication, Characterization, and Photovoltaic Application. *ACS Nano* **2011**, *5*, 6629–6636.

(20) Plass, K. E.; Filler, M. A.; Spurgeon, J. M.; Kayes, B. M.; Maldonado, S.; Brunschwig, B. S.; Atwater, H. A.; Lewis, N. S. Flexible Polymer-Embedded Si Wire Arrays. *Adv. Mater.* **2009**, *21*, 325–328.

(21) Li, X. Y.; Tao, J. A.; Guo, W. X.; Zhang, X. J.; Luo, J. J.; Chen, M. X.; Zhu, J.; Pan, C. F. A Self-Powered System Based on Triboelectric Nanogenerators and Supercapacitors for Metal Corrosion Prevention. *J. Mater. Chem. A* **2015**, *3*, 22663–22668.

(22) Xue, F.; Chen, L. B.; Chen, J.; Liu, J. B.; Wang, L. F.; Chen, M. X.; Pang, Y. K.; Yang, X. N.; Gao, G. Y.; Zhai, J. Y.; Wang, Z. L. p-Type MoS₂ and n-Type ZnO Diode and Its Performance Enhancement by the Piezophototronic Effect. *Adv. Mater.* **2016**, *28*, 3391–3398.

(23) Moon, T.; Chen, L.; Choi, S.; Kim, C.; Lu, W. Efficient Si Nanowire Array Transfer via Bi-Layer Structure Formation Through Metal-Assisted Chemical Etching. *Adv. Funct. Mater.* **2014**, *24*, 1949–1955.

(24) Xu, S.; Xu, C.; Liu, Y.; Hu, Y. F.; Yang, R. S.; Yang, Q.; Ryou, J. H.; Kim, H. J.; Lochner, Z.; Choi, S.; Dupuis, R.; Wang, Z. L. Ordered Nanowire Array Blue/Near-UV Light Emitting Diodes. *Adv. Mater.* **2010**, *22*, 4749–4753.

(25) Pan, C. F.; Dong, L.; Zhu, G.; Niu, S. M.; Yu, R. M.; Yang, Q.; Liu, Y.; Wang, Z. L. High-Resolution Electroluminescent Imaging of Pressure Distribution Using a Piezoelectric Nanowire LED Array. *Nat. Photonics* **2013**, *7*, 752–758.

(26) Huang, Y. M.; Ma, Q. L.; Zhai, B. G. Wavelength Tunable Photoluminescence of ZnO/Porous Si Nanocomposites. *J. Lumin.* **2013**, *138*, 157–163.

(27) Chan, Y. F.; Su, W.; Zhang, C. X.; Wu, Z. L.; Tang, Y.; Sun, X. Q.; Xu, H. J. Electroluminescence from ZnO-Nanofilm/Si-Micropillar Heterostructure Arrays. *Opt. Express* **2012**, *20*, 24280–24287.

(28) Ye, J. D.; Gu, S. L.; Zhu, S. M.; Liu, W.; Liu, S. M.; Zhang, R.; Shi, Y.; Zheng, Y. D. Electroluminescent and Transport Mechanisms of n-ZnO/p-Si Heterojunctions. *Appl. Phys. Lett.* **2006**, *88*, 182112.

(29) Lee, S. W.; Cho, H. D.; Panin, G.; Kang, T. W. Vertical ZnO Nanorod/Si Contact Light-Emitting Diode. *Appl. Phys. Lett.* **2011**, *98*, 093110.

(30) Park, N. M.; Kim, T. S.; Park, S. J. Band Gap Engineering of Amorphous Silicon Quantum Dots for Light-Emitting Diodes. *Appl. Phys. Lett.* **2001**, *78*, 2575–2577.

(31) Koshida, N.; Koyama, H. Efficient Visible Photoluminescence from Porous Silicon. *Jpn. J. Appl. Phys., Part 2* **1991**, *30*, L1221–L1223.

(32) Maier-Flaig, F.; Rinck, J.; Stephan, M.; Bocksrocker, T.; Bruns, M.; Kubel, C.; Powell, A. K.; Ozin, G. A.; Lemmer, U. Multicolor Silicon Light-Emitting Diodes (SiLEDs). *Nano Lett.* **2013**, *13*, 475–480.

(33) Aspetti, C. O.; Cho, C. H.; Agarwal, R.; Agarwal, R. Studies of Hot Photoluminescence in Plasmonically Coupled Silicon via Variable Energy Excitation and Temperature-Dependent Spectroscopy. *Nano Lett.* **2014**, *14*, 5413–5422.

(34) Pan, C. F.; Niu, S. M.; Ding, Y.; Dong, L.; Yu, R. M.; Liu, Y.; Zhu, G.; Wang, Z. L. Enhanced Cu₂S/CdS Co Axial Nanowire Solar Cells by Piezo-Phototronic Effect. *Nano Lett.* **2012**, *12*, 3302–3307.

(35) Yang, Q.; Liu, Y.; Pan, C. F.; Chen, J.; Wen, X. N.; Wang, Z. L. Largely Enhanced Efficiency in ZnO Nanowire/p-Polymer Hybridized Inorganic/Organic Ultraviolet Light-Emitting Diode by Piezo-Phototronic Effect. *Nano Lett.* **2013**, *13*, 607–613.

(36) Yang, Q.; Wang, W. H.; Xu, S.; Wang, Z. L. Enhancing Light Emission of ZnO Microwire-Based Diodes by Piezo-Phototronic Effect. *Nano Lett.* **2011**, *11*, 4012–4017.

(37) Han, X.; Du, W. M.; Yu, R. M.; Pan, C. F.; Wang, Z. L. Piezo-Phototronic Enhanced UV Sensing Based on a Nanowire Photodetector Array. *Adv. Mater.* **2015**, *27*, 7963–7969.

(38) Bao, R. R.; Wang, C. F.; Dong, L.; Yu, R. M.; Zhao, K.; Wang, Z. L.; Pan, C. F. Flexible and Controllable Piezo-Phototronic Pressure Mapping Sensor Matrix by ZnO NW/p-Polymer LED Array. *Adv. Funct. Mater.* **2015**, *25*, 2884–2891.

(39) Chen, M. X.; Pan, C. F.; Zhang, T. P.; Li, X. Y.; Liang, R. R.; Wang, Z. L. Tuning Light Emission of a Pressure-Sensitive Silicon/ZnO Nanowires Heterostructure Matrix through Piezo-Phototronic Effects. *ACS Nano* **2016**, *10*, 6074–6079.